

tune shift, and perhaps other measures to prevent the beam from becoming too cold at the injection energy;

- detectors at small angles see a beam halo. While the rates are less than would be seen for a comparable detector in a cyclotron beam line, they are troublesome at present luminosities and may limit some experiments at the higher luminosities expected in future operation. Attempts to limit the small angle rate with cleanup slits and scrapers elsewhere in the ring have not yet been very successful. A better understanding of the tail of the beam distribution is required.

To summarize, the Cooler is now contributing to the research output of the laboratory and drawing interest from a growing fraction of our user community. Exploration of the parameter space of Cooler operation has defined the boundaries of a quite wide region available now for research use. Further extensions of the boundaries are possible. Work toward this end is resource-limited and is largely concentrated on the needs of experiments in the pipeline: diversity of target technologies; maximum event rates and the quietest possible environment for the detectors clustered around internal targets.

COOLER INTENSITY LIMITATIONS

Tim Ellison

Indiana University Cyclotron Facility, Bloomington, IN 47408

I. Introduction

The combination of our ability, based upon experience, to produce better ramp waveforms, our Cool-Ramp-Cool capabilities, and the new beam phase feedback system, now allow us to accelerate beams with very high efficiency, approaching 100%. The maximum stored beam current at high energies (≈ 1 mA) is now limited by instabilities at the low energy used for stripping injection (90 MeV H_2^+). The simplest way to increase the threshold currents for instabilities is to simply not cool the injected beam (as is being done at Uppsala and will be done in COSY) since the threshold current for instabilities increases with the beam emittance, momentum spread and beam energy. However, due to the low current of our injector, we need electron cooling to accumulate beam up to the level where instabilities are observed. Consequently, we need to learn to operate in a mode where we take advantage of cooling to accumulate beam, but avoid the accompanying problems associated with these low equilibrium emittance and momentum spread beams. Thus far we have identified two limitations: coherent transverse instabilities and the space charge tune shift. Below we briefly discuss each of these limitations, and the work we will be doing to alleviate them.

II. Coherent Transverse Instabilities

M. Ball, D.D. Caussyn, T. Ellison, B. Hamilton, and S.Y. Lee

We encounter coherent transverse instabilities for coasting beam currents in the range from about 0.5 to 5 mA. A textbook example of a such an instability is shown in Fig. 1. The signal shown in the upper trace of Fig. 1 can be examined to determine the mode number of the instability by using either a spectrum analyzer tuned to a specific betatron sideband, or an oscilloscope operating with a much faster sweep rate. Fig. 2 shows an expanded view of the signal in the upper trace of Fig. 1; in this case, the mode number is 2. (The observed frequency is $(Q_x - 2)f_o$, where Q_x is the horizontal betatron tune ($\times 3.7$), and f_o is the revolution frequency. This corresponds to the following picture. If an instantaneous snapshot of the beam transverse position were made at all locations around the ring, one would see, superimposed upon the closed orbit error, a frequency and amplitude modulated sinusoidal pattern making two complete cycles).

We are building a transverse beam damping system to suppress these instabilities. The instability exponential growth rate is about 10 ms. In the first test of our damping system, we were able to damp deliberately-induced coherent oscillations in about 1 ms (see Fig. 3). This system, however, was only able to increase the threshold current for instabilities by less than 50%. We think this is principally due to the fact that the system bandwidth is not low enough to correct for about the 4 lowest frequency modes. While operating with the dampers, we observed the amplitude of the low-mode-number, undamped instabilities to

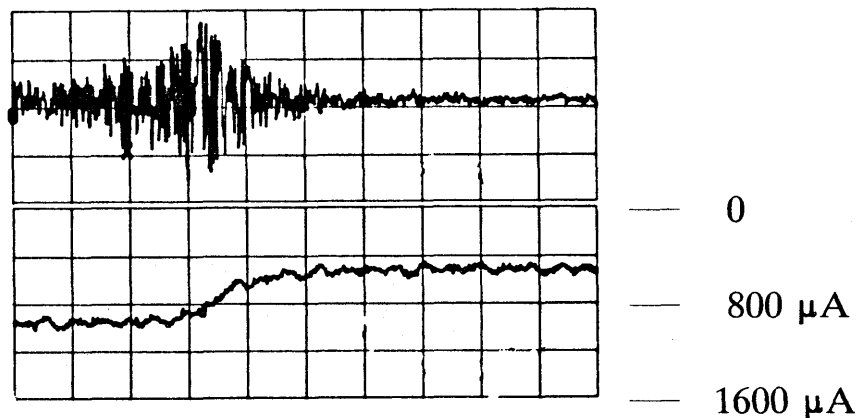


Figure 1. The upper oscilloscope trace records the difference signal (proportional to the product of the beam position and intensity) from a beam position electrode at the onset of the instability. The lower trace shows the resulting decrease in beam intensity, as recorded by the PCT (50 ms/div).

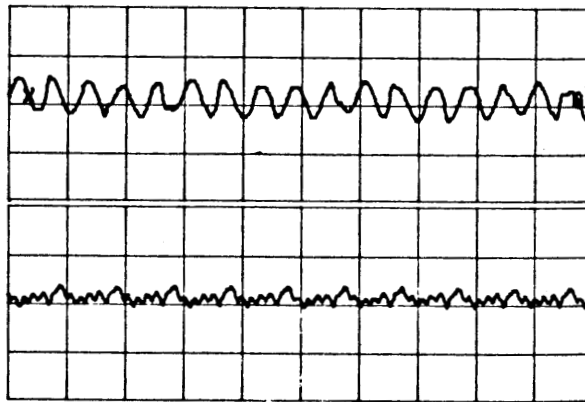


Figure 2. The Difference (top) and Sum (bottom) signals from a horizontal BPM (beam position electrode); both signals have the same total gain; $1 \mu\text{s}$ (≈ 1 orbital revolution period) per division. In the upper trace one observes the $(Q_x - 2)f_o$ instability. In the lower trace, one sees a small amount of longitudinal self bunching at the 1st and 5th harmonic; the rf cavity is shorted.

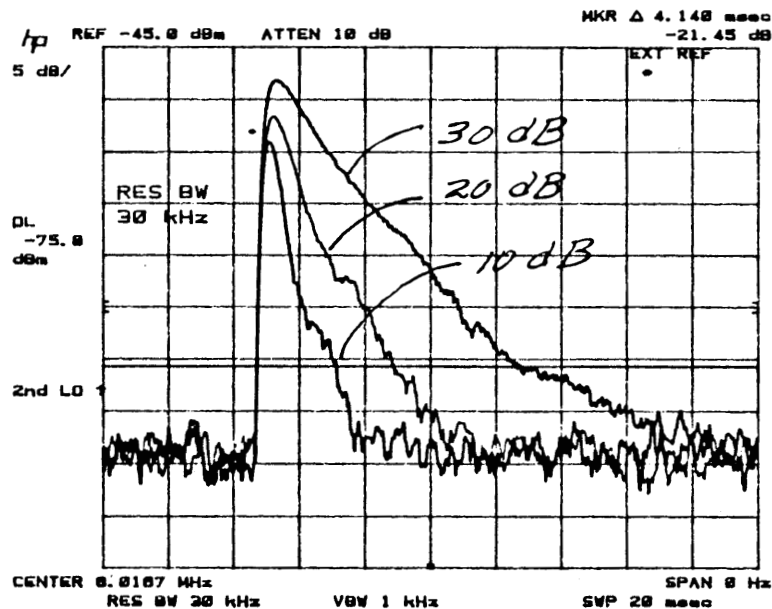


Figure 3. Betatron amplitude vs. time as a function of attenuation in the damper system. (2 ms/div; 5 dB ($\times 1.78$)/div).

increase exponentially in coincidence with beam loss (see Fig. 4). (The lowest order modes are the most important, since the threshold current for transverse instabilities increases approximately linearly with mode number. In addition, the natural damping time for these low frequency modes is extremely long since the product of the chromaticity and tune is approximately equal to the mode number.) New amplifiers, with a much lower low-frequency cutoff will be installed in the summer of 1991.

Besides damping instabilities, these dampers may allow us to substantially increase the rate at which we can stack beams (limited in certain regimes by transverse heating from the injection kickers) and allow us to try techniques to ameliorate others problems, such as the space charge tune shift (i.e., without dampers we cannot use noise to increase the transverse beam size and consequently reduce the space charge tune shift, without inducing coherent transverse instabilities).

In addition to this damping system, we shall also try other techniques to increase the threshold current for these instabilities. One such technique we will try in the near future is to use the sextupoles to increase the change in betatron tune with betatron amplitude.

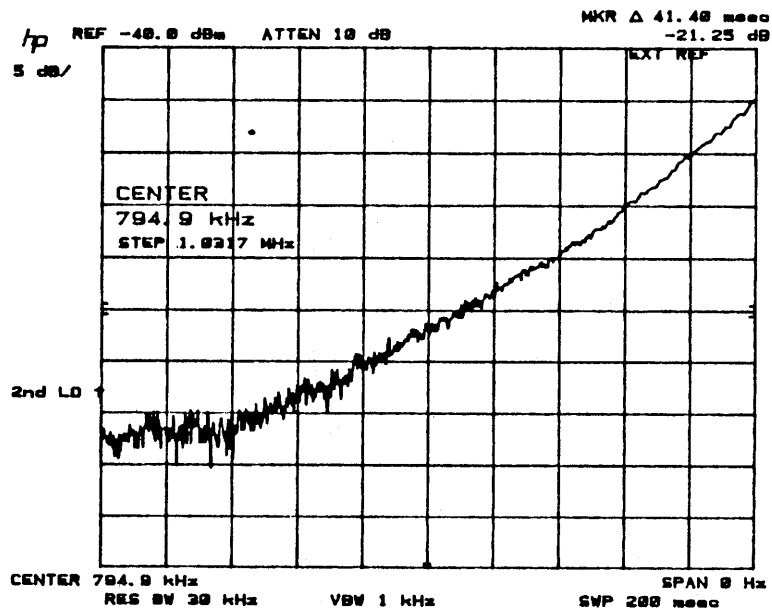


Figure 4. Exponential growth of the undamped $(Q_x - 3)f_o$ (≈ 0.78 MHz) mode just prior to beam loss. (20 ms, 5 dB ($\times 1.78$)/div).

III. Estimation of the Beam Space Charge Tune Shift in the Cooler

M. Ball, D.D. Caussyn, J. Collins, V. Derenchuk, D. DuPlantis, G. East,
T. Ellison, D. Friesel, B. Hamilton, B. Jones, S.Y. Lee, M. G. Minty, and T. Sloan

We have also experienced intensity limits without observing any of the coherent transverse instabilities mentioned above. Clearly, in addition to coherent transverse instabilities, at least one other process limits the beam current. One such possible process is the space-charge tune shift. To assess the likelihood of this process playing a role in limiting intensity, the bunching factor and the beam emittance were measured for a stored 45 MeV proton beam cooled with a 0.72 A electron beam and used to calculate the space-charge tune shift.

The bunching factor, B_f , is a measure of the peak-to-average beam current. Assuming that the beam distribution is Gaussian, we define $B_f (> 1)$ by

$$B_f = \frac{\tau}{\sqrt{2\pi}\sigma_t}, \quad (1)$$

where τ is the rf period, and σ_t is the time width of the beam. The value of σ_t was measured from the oscilloscope trace of the signal from a beam position monitor (BPM), or the low bandwidth or high bandwidth wall gap monitor, whichever of the three had the most suitable bandwidth for the beam pulse width. Generally, we observed that the B_f decreases with increasing beam current and does not appear to have a strong dependence on the quality of the electron cooling. These measurements are summarized in Fig. 5.

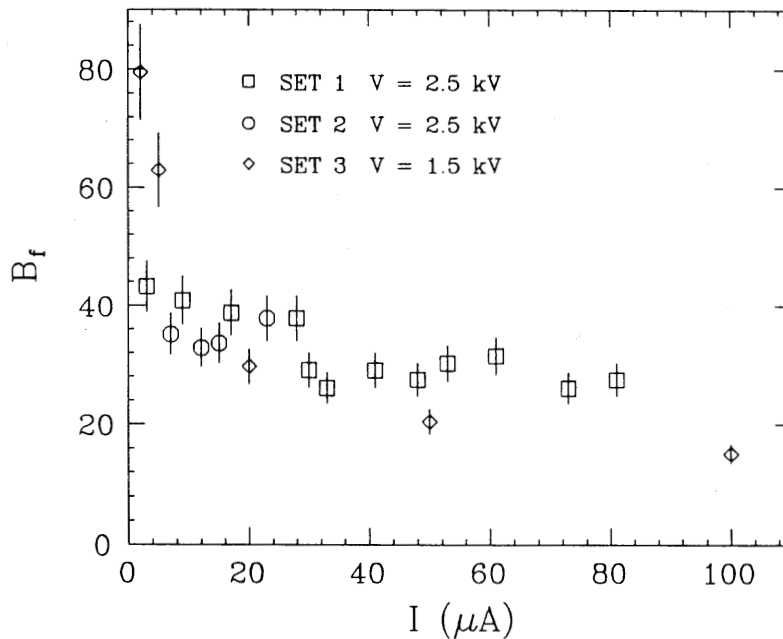


Figure 5. Measured bunching factor as a function of beam current ($h=6$, $V_{rf} = 2$ kV).

The horizontal transverse emittance, ϵ_x , is found from the width of the beam profile. The profile was determined by horizontally sweeping the beam through a vertically-mounted $10 \mu\text{m}$ diameter carbon fiber and measuring the secondary emission current while simultaneously measuring the position of the beam centroid using a nearby beam position monitor, BPM.

The width of the beam profile, σ_x , includes a contribution due to betatron oscillations, $\sigma_{x\beta}$, and another due to the beam momentum spread and the ring dispersion, σ_{xp} . For an electron cooled proton beam, the Fokker-Planck equation gives basically a Gaussian distribution in the six dimensional phase space. In this case, the rms beam size is given by the Gaussian quadrature of the components from momentum and position space, and the broadening due to the momentum spread can be removed. Then, the transverse emittance is calculated using the relation, $\epsilon_x = \sigma_{x\beta}^2 / \beta_x$, where β_x is the betatron amplitude function ($\beta_x = 2.0 \text{ m}$). We assume the horizontal and vertical beam size to be the same.

In Fig. 6, values of $\sigma_{x\beta}$ are plotted versus the relative angular misalignment of the electron and proton beams in the electron cooling region. The misalignment was produced by "tilting" the magnetic field lines in the cooling region solenoid by varying the strength of a superimposed horizontal dipole magnetic field. All the data in this figure were taken with identical operating conditions with the exception of the point marked with a diamond for which there is an additional insignificant vertical misalignment.

It is clear from Fig. 6 that ϵ_x is a strong function of the electron/proton beam alignment. In fact, for a large part of the range covered by the data, the equilibrium proton beam rms divergence in the cooling region is, to good approximation, the angular misalignment between the electron and proton beams.

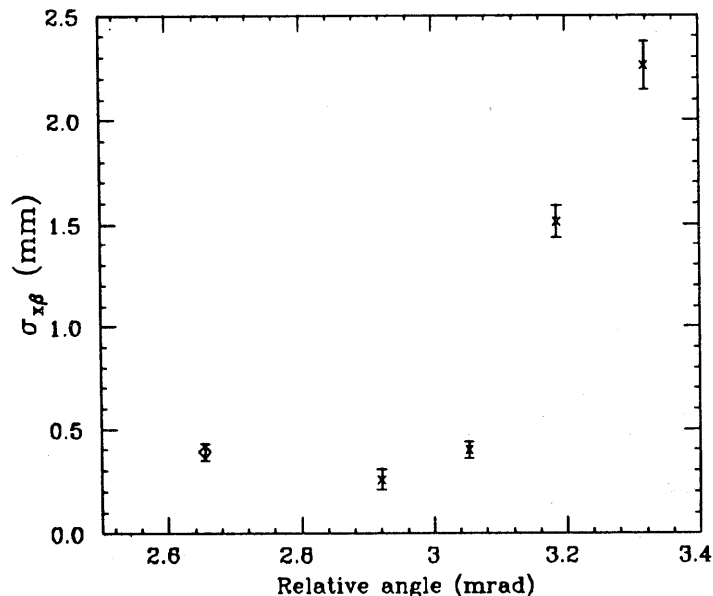


Figure 6. Plot of the rms beam width due to betatron oscillations versus relative angular misalignment of the proton and electron beams in the cooler region. Note that the location of the origin for the angular misalignment is arbitrary.

In Fig. 7, values of ϵ_x are plotted as a function of beam current for each of the three sets of data taken. The electron cooling (beam alignment) is improved in moving from the first to the third data set. With a possible exception for beam currents less than $20 \mu\text{A}$, ϵ_x generally increases with beam current. There is also a systematic decrease in emittance in going from the first to the third data set corresponding to the improved cooling.

Assuming that the beam is on-axis in a circular chamber with negligible effects due to image charges and currents, the space-charge tune shift is calculated from,²

$$\nu_{sc} = -\frac{NRr_p}{\pi\nu_x\gamma^3\beta^2} \frac{B_f\beta_x}{4\epsilon_x}. \quad (2)$$

In this expression, N is the number of particles in the ring, R is the ring radius, r_p is the classical proton radius, ν_x is the horizontal betatron tune of the cooler ring, and β and γ are the usual relativistic factors. The ν_x for the ring was measured using the ping-tune method,¹ and was about 3.8. Values calculated for the magnitude of $\Delta\nu_{sc}$ are plotted versus beam current in Fig. 8 for each of the three data sets discussed previously. In this figure it is evident that $|\Delta\nu_{sc}|$ monotonically increases with beam current. It is also clear that as the cooling is improved, the values of $|\Delta\nu_{sc}|$ are greater at each current. It is also suggestive that $|\Delta\nu_{sc}|$ increases with beam current at greater rates as cooling is improved.

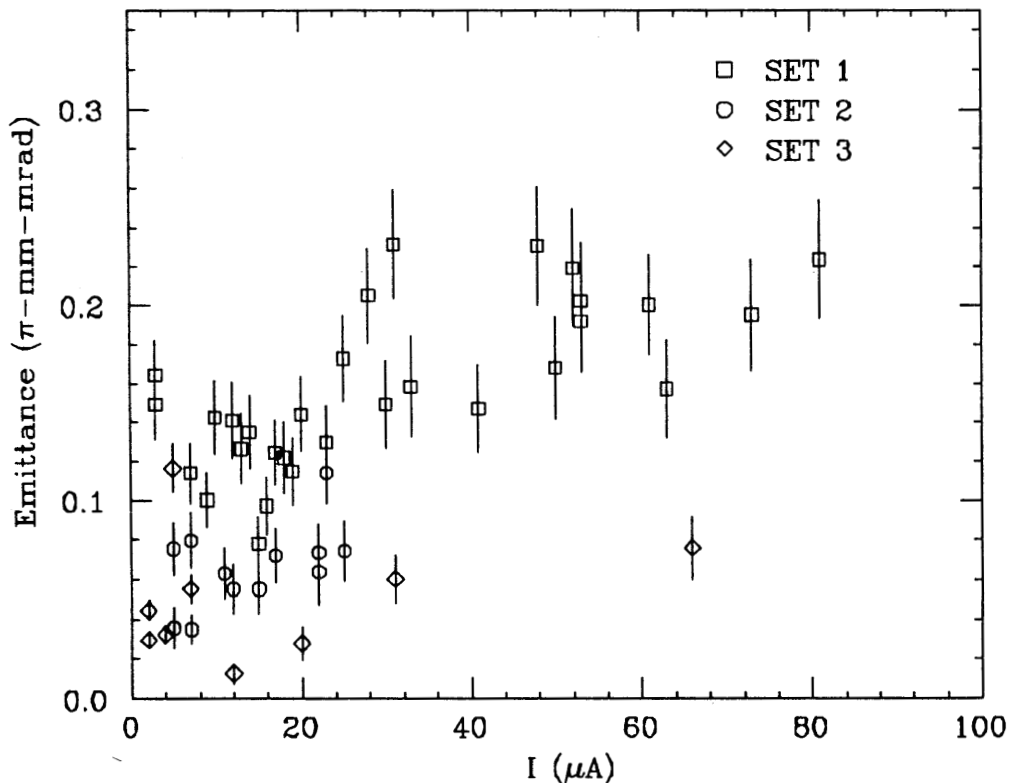


Figure 7. Plot of the radial transverse emittance versus beam current for data taken with three slightly different operating conditions.

In conclusion, we have found that the transverse emittance is very sensitive to the angular alignment between the electron and proton beams within the electron cooling region. The longitudinal emittance, as evidenced by the bunching factor, is less sensitive. Over the range of stored beam currents explored here, we have seen calculated space-charge tune shifts in a broad range, but increasingly large when the misalignment between the electron and proton beam is minimized. The magnitude of the observed tune shifts were as large as 0.3 with the best cooling. With higher currents and optimized cooling, larger space-charge tune shifts are expected. With tune shifts of this magnitude, it is evident that space charge is indeed a factor in stored beam current limitations observed in the IUCF Cooler. Additional studies in which the beam lifetime corresponding to these large tuneshifts is measured, and more precise measurements of emittance is made, would be useful. From a more practical perspective, we would like to learn how to increase the equilibrium emittance in a controlled manner (to reduce the space charge tune shift) without decreasing the cooling rate (needed for high accumulation rates).

1. M. Ball, D.D. Caussyn, T. Ellison, B. Hamilton, N. Yoder, "A beam tracking system for use in orbital dynamics," this report.
2. B. Zotter, "Betatron frequency shifts due to image and self fields," in *CERN Accelerator School, General Accelerator Physics*, eds. P. Bryant, S. Turner, CERN 85-19, p. 253.

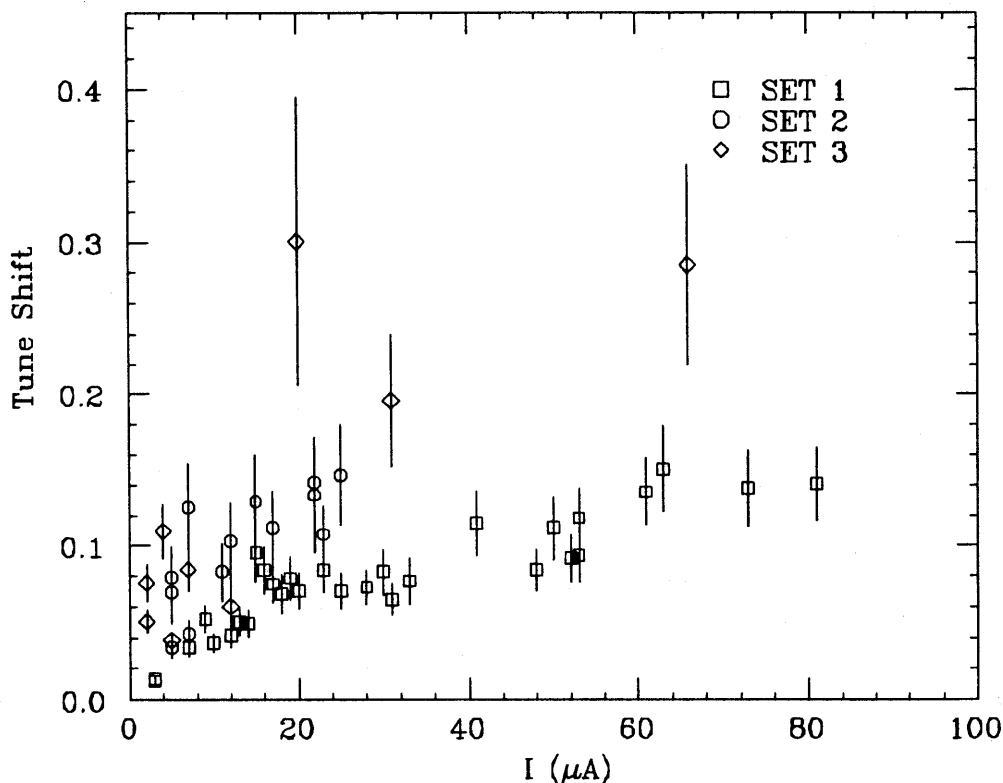


Figure 8. Plot of calculated space-charge tune shift versus beam current.